Letter

First-order transitions in spin chains coupled to quantum baths

C. A. Perroni,[1] A. De Candia,[1,2] V. Cataudella,[1] R. Fazio,[1,3,4] and G. De Filippis[1]
[1]*CNR-SPIN and Physics Department E. Pancini, Università degli Studi di Napoli Federico II, Complesso Universitario Monte S. Angelo, Via Cintia, I-80126 Napoli, Italy*
[2]*INFN, Sezione di Napoli, Complesso Universitario di Monte S. Angelo, I-80126 Napoli, Italy*
[3]*International Centre for Theoretical Physics, Strada Costiera 11, I-34151 Trieste, Italy*
[4]*National Enterprise for nanoScience and nanoTechnology, Istituto Nanoscienze-CNR, I-56126 Pisa, Italy*

(Received 4 August 2022; revised 28 February 2023; accepted 1 March 2023; published 10 March 2023)

We show that tailoring the dissipative environment allows us to change the features of continuous quantum phase transitions and even induce first-order transitions in ferromagnetic spin chains. In particular, using a numerically exact quantum Monte Carlo method for the paradigmatic Ising chain of one-half spins in a transverse magnetic field, we find that spin couplings to local quantum boson baths (in the Ohmic regime) can drive the transition from the second to the first order even for a low dissipation strength. Moreover, using a variational mean-field approach for the treatment of spin-spin and spin-boson interactions, we point out that phase discontinuities are ascribable to a dissipation-induced effective magnetic field which is intrinsically related to the bath quantum fluctuations and vanishes for classical baths. The effective field is able to switch the sign of the magnetization along the direction of spin-spin interactions. The results can be potentially tested in recent quantum simulators and are relevant for quantum sensing since the spin system could not only detect the properties of nonclassical baths, but also the effects of weak magnetic fields.

DOI: 10.1103/PhysRevB.107.L100302

Introduction. A quantum phase transition (QPT) occurs at zero temperature when quantum fluctuations, tuned through a physical parameter, such as a magnetic field, are able to induce a sudden change in the ground state of a system with many-body interactions [1]. The behavior of static quantities at QPT is typically obtained at the thermodynamic equilibrium by exploiting the quantum-to-classical mapping, that is, the mapping to a classical statistical model with an additional imaginary-time dimension [1]. Most studied QPTs are continuous [1,2]. A paradigmatic example is provided by the Ising chain of one-half spins where the increase of a transverse magnetic field induces the change from an ordered ferromagnetic to a paramagnetic disordered phase [3]. Attention has recently focused also on first-order QPTs [2] whose large sensitivity to external perturbations can be exploited for sensing applications.

Any quantum system is inevitably coupled to the environment whose interactions can significantly change physical features. Then the fundamental question is as follows: How does the coupling with its surroundings affect a system close to a QPT? To this aim two different routes have been proposed in the literature. In the former one, the steady state reached by the system coupled to Markovian baths has been investigated starting from a Lindblad master equation [4,5]. In the latter one, dissipation is explicitly introduced by modeling the environment as an infinite set of harmonic quantum oscillators [5–7]. Within this approach, the entire universe (system+environment) is considered at thermodynamical equilibrium. Of course, this does not imply any assumption for the system stationary state. As a further consequence, non-Markovian effects can be fully included [8]. In the following we will focus our attention on this second proposal.

The recent realization of programmable spin models with tunable interactions [9–11] has stimulated an intense theoretical study of the transverse field Ising model in the presence of dissipation [12]. In some studies of this model, the environment is accurately modeled as an infinite set of local boson baths. Indeed, each spin is coupled to an infinite number of oscillators giving rise to the well-known spin-boson model [6,7,13]. In the Ohmic case, quantum Monte Carlo (QMC) studies have shown that these dissipative mechanisms can drive QPTs even in the case of a single-spin system [13–15]. For many-body systems, nonperturbative properties depend in a crucial way on the specific coupling with the bath. Indeed, for the quantum Ising chain coupled to oscillator baths [16–18], when spin-bath couplings are along the direction of spin-spin interactions, the dynamical critical exponent changes while the transition remains continuous.

In this Letter, the spin-bath interaction is further tailored with the aim to induce first-order transitions. In particular, we study zero-temperature stationary properties of the transverse field Ising chain with one-half spins coupled to bosonic local baths in the Ohmic regime through a term which, for a single spin, is a combination of Jaynes-Cummings and anti-Jaynes-Cummings interactions [19,20]. We remark that these spin-bath couplings have been previously analyzed, limited to the case of a single spin with a single oscillator. We stress that, in the present Letter, for each spin there is a local bath, each made of a large number of oscillators. This is completely different from the situation, analyzed for example in Ref. [14] by some of us, where there is only one global bath for all the spins in the chain. We use the numerically exact QMC method up to the thermodynamic limit showing that the spin couplings considered in this work are able to drive the phase transition

from the second to the first order also for a low dissipation strength. Following previous studies [16–18], we focus on the effects due to Ohmic baths, however, the change of the order of the transition is quite robust to other kinds of baths, such as sub-Ohmic or super-Ohmic ones.

Moreover, we develop a semianalytical zero-temperature variational mean-field (VMF) approach which is in very good agreement with the QMC method, clarifying that phase discontinuities are present only for quantum baths. In fact, the VMF approach highlights the role played by a dissipation-induced effective magnetic field which switches its sign along the direction of spin-spin interactions with varying the properties of the bath. Finally, we point out that the strong sensitivity of the spin system to the properties of nonclassical baths at minimal coupling and to the strength of the magnetic field could be exploited in phenomena relevant for the realization of small-scale quantum sensors.

The model. The Hamiltonian is

$$H = H_S + H_B + H_{SB}, \tag{1}$$

where H_S describes the spin couplings within the Ising chain in a transverse field [3]

$$H_S = \frac{\Delta}{2}\sum_{i=1}^{L}\sigma_i^x - \frac{J}{4}\sum_{i=1}^{L-1}\sigma_i^z\sigma_{i+1}^z, \tag{2}$$

with the energy Δ providing the strength of the transverse field along the x direction, the energy J the exchange couplings of spins along the z direction, $i = 1, \ldots, L$, indicating the L sites of the chain, σ_i^x, σ_i^z the Pauli matrices on each chain site with eigenvalues $1, -1$. In Eq. (1), the Hamiltonian H_B describes L local baths, each one being associated to one of the L sites i,

$$H_B = \sum_{i=1}^{L}\sum_{k}\hbar\omega_k a_{i,k}^{+}a_{i,k}, \tag{3}$$

where $a_{i,k}^{+}$ ($a_{i,k}$) creates (destroys) the boson mode k of the bath at the site i. All the local baths are assumed to have the same frequency spectrum ω_k (independent of the site i). Finally, the spin-bath coupling combines Jaynes-Cummings (rotating) and anti-Jaynes-Cummings (counterrotating) interactions [19,20] through the dimensionless bath parameter γ,

$$H_{SB} = \sum_{i=1}^{L}\sum_{k}\lambda_k\{a_{i,k}[\gamma\sigma_i^{-} + (1-\gamma)\sigma_i^{+}] + \text{H.c.}\}, \tag{4}$$

where the bath spectral function $F(\omega)$ is defined in terms of the couplings λ_k: $F(\omega) = \sum_k \lambda_k^2\delta(\omega_k - \omega) = \frac{\alpha\hbar}{2}\omega_c^{1-\nu}\omega^{\nu}\Theta(\omega_c - \omega)$, which is proportional to the dimensionless spin-bath coupling constant α. Unless otherwise stated, we take $\hbar = 1$, $\Delta = 1$, cutoff energy $\omega_c = 10$. In addition to the coupling strength α, a very important parameter characterizing the bath is ν [13]. Actually, $\nu = 1$ corresponds to the most studied Ohmic baths, $\nu < 1$ to sub-Ohmic ones, $\nu > 1$ to super-Ohmic ones. In analogy with previous studies [16–18], the focus of the work will be on Ohmic baths.

The QMC approach. The QMC method consists of quantum-to-classical mapping with the introduction of an additional imaginary-time dimension, exact integration of boson bath degrees of freedom, and MC simulation of the resulting system spin action up to the thermodynamic limit [1].

For the first step, we use the Suzuki-Trotter approximation [3] writing the partition function as $\mathrm{Tr}(e^{-\beta H}) = \sum_{\{\phi_1,\phi_N\}}\langle\phi_1|e^{-\frac{\beta}{N}H}|\phi_2\rangle\cdots\langle\phi_N|e^{-\frac{\beta}{N}H}|\phi_1\rangle$, where $|\phi_j\rangle$ is the state of the system (both spins and bosons degrees of freedom) at the jth imaginary time. We therefore obtain a classical system in $(1+1)$ dimensions, where $S_{i,j} = \pm 1$ is the value of the spin at site $i = 1 \ldots L$ and time $j = 1 \ldots N$. For each site i and pair of imaginary times j, j', we introduce an auxiliary variable $b_{i,j,j'} = 0, 1$ that is equal to 1 if a phonon is emitted and absorbed at j and j', 0 otherwise.

After summing over the phonon degrees of freedom, the weight of a configuration $\{S_{i,j}, b_{i,j,j'}\}$ is given by

$$\begin{aligned} W(\{S_{i,j}, b_{i,j,j'}\}) = {} & \exp[-\mathcal{H}_{\mathrm{nn}}(\{S_{i,j}\})] \\ & \times \prod_{i,j}\left(\delta_{B_{i,j},0} + \delta_{S_{i,j},-S_{i,j+1}}\delta_{B_{i,j},1}\right) \\ & \times \prod_{j'>j}\left[\frac{4}{\Delta^2}K_{S_{i,j},S_{i,j'}}\left(\frac{\beta}{N}|j'-j|\right)\right]^{b_{i,j,j'}}, \end{aligned} \tag{5}$$

where $\mathcal{H}_{\mathrm{nn}}(\{S_{i,j}\})$ is a nearest-neighbor classical Hamiltonian induced by the quantum Hamiltonian (1),

$$\mathcal{H}_{\mathrm{nn}}(\{S_{i,j}\}) = \sum_{i=1}^{L}\sum_{j=1}^{N}(-J_\tau S_{i,j}S_{i,j+1} - \tilde{J}S_{i,j}S_{i+1,j}), \tag{6}$$

with $J_\tau = -\frac{1}{2}\ln(\frac{\tau\Delta}{2})$, $\tilde{J} = \frac{\tau J}{4}$, couplings along the time and spatial directions, respectively, and periodic boundary conditions in the time direction. The variables $B_{i,j}$ are defined as $B_{i,j} = \sum_{j'} b_{i,j,j'}$, and are limited to values 0 and 1 in the limit $N \to \infty$, since larger values are suppressed by factors β/N. The long-range kernel $K_{s,s'}(\tau)$ is given by

$$K_{s,s'}(\tau) = \begin{cases} \gamma^2\tilde{K}_s(\tau) + (1-\gamma)^2\tilde{K}_{s'}(\tau), & \text{if } s \neq s', \\ \gamma(1-\gamma)[\tilde{K}_1(\tau) + \tilde{K}_{-1}(\tau)], & \text{if } s = s', \end{cases}$$

with

$$\tilde{K}_s(\tau) = \int_0^{\infty} d\omega\, F(\omega)\frac{e^{s\omega(\tau-\frac{\beta}{2})}}{e^{\omega\beta/2} - e^{-\omega\beta/2}}.$$

Note that, for $\gamma \neq \frac{1}{2}$, the kernel $K_{s,s'}$ breaks the Z_2 symmetry, since $K_{1,-1}(\tau) \neq K_{-1,1}(\tau)$. In particular, for $\gamma > \frac{1}{2}$, configurations with negative magnetization m_z are favored, while for $\gamma < \frac{1}{2}$, it is the opposite. Finally, in the classical limit, the function $\tilde{K}_s(\tau)$ becomes constant and independent of s: $\tilde{K}_s(\tau) = \frac{\alpha\omega_c}{2\beta}$, so that the Z_2 symmetry is restored [21].

We point out that breaking of Z_2 symmetry is quite general for quantum baths, such as sub-Ohmic or super-Ohmic, as long as γ is different from $1/2$. Likewise, restoration of Z_2 symmetry is valid for different kinds of classical baths. Therefore, we believe the main findings of our work do not qualitatively change with varying the features of the quantum baths. Of course, at $\gamma = 1/2$, the universality class of the continuous transition could depend on the kind of quantum bath [13].

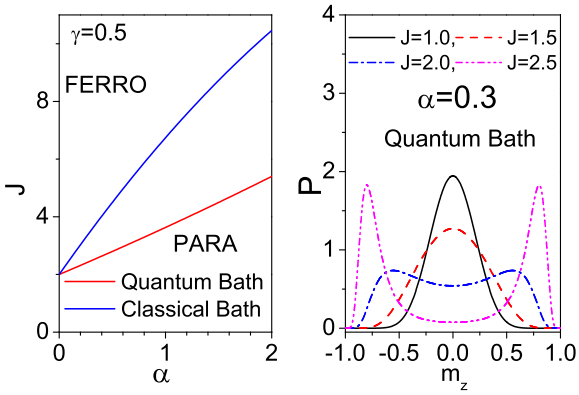

FIG. 1. Left panel: Phase diagram with J vs α for $\gamma = 0.5$ in the case of both quantum and classical baths. FERRO stands for the ferromagnetic, and PARA for the paramagnetic phase. Right panel: Distribution function P as a function of the magnetization m_Z for different values of J in the case of quantum baths at $\gamma = 0.5$ and $\alpha = 0.3$ (critical $J_c = 2.47$). QMC simulation parameters for the right panel: $L = 10$, and $\beta = 10$.

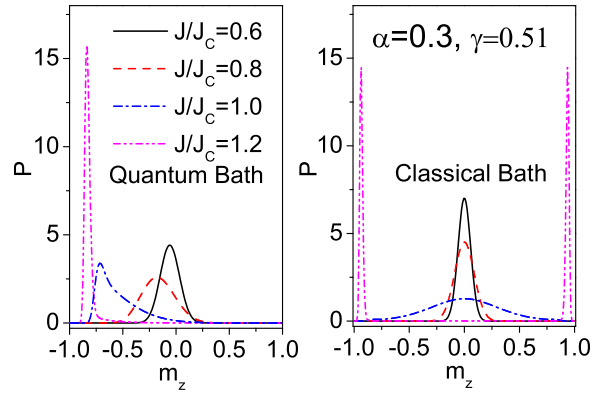

FIG. 2. Distribution function P as a function of the magnetization m_Z for different values of J in the case of quantum (left panel) and classical baths (right panel) for $\alpha = 0.3$ and $\gamma = 0.51$. QMC simulation parameters: $L = 10$, and $\beta = 100$.

The left panel of Fig. 1 shows the phase diagram for $\gamma = \frac{1}{2}$ obtained by using Binder cumulants [21]. For $\alpha = 0$, QMC results recover the well-known critical value $J_c = 2$ for the transition from the paramagnetic to ferromagnetic phase [3]. The local spin operator in the spin-bath Hamiltonian (4) becomes $\gamma\sigma_i^- + (1-\gamma)\sigma_i^+ = \sigma_i^x/2$, therefore it is along the direction x as the transverse field Δ in Eq. (2). Clearly, at $J = 0$ (case of a single spin), only the paramagnetic phase is stable. Indeed, the single-spin model is exactly solved, and it does not present any delocalized-localized transition of Kosterlitz-Thouless type with increasing α [14,22]. For finite J larger than J_c, we always find a second-order transition from a paramagnetic to a ferromagnetic phase as a function of α. Indeed, the critical J_c gets enhanced with increasing α along a transition line quite sensitive to system parameters. Moreover, as detailed in the Supplemental Material, the dynamical critical exponent z is always equal to 1 with changing α, in analogy with QMC results in Ising chains with Ohmic bond dissipation [23]. Therefore, our results differ from those of the QMC literature [16–18] where σ_i^z is the local spin operator mediating the interaction with quantum local baths [24]. QMC results for $\gamma = \frac{1}{2}$ can be interpreted within the VMF approach, introduced below, in terms of an enhancement, proportional to α, of an effective transverse magnetic field.

As discussed in the Supplemental Material [21], classical baths provide more intense effective transverse magnetic fields. The left panel of Fig. 1 shows that, as expected, the classical baths are more effective in contrasting ferromagnetic correlations. Indeed, at fixed J, the critical α to the paramagnetic phase is smaller for classical baths. Therefore, at $\alpha = 0.3$, $J_c = 2.47$ for quantum baths, while $J_c = 3.67$ for classical baths. In particular, for the case of quantum baths, in the right panel of Fig. 1, we plot the distribution function P as a function of the magnetization m_Z along the z axis for values of J smaller and slightly larger than J_C. Actually, as expected for systems with Z_2 symmetry, the function P is symmetric around zero and shows a change from a monomodal to a bimodal character with crossing J_C.

More interesting QMC results are obtained for $\gamma \neq \frac{1}{2}$ where quantum bath fluctuations break Z_2 symmetry. For $J = 0$ (single-spin case) the transition from a delocalized to localized phase is still absent with increasing α, in analogy with the case $\gamma = \frac{1}{2}$ [25]. However, we find different results about the magnetic behavior. Indeed, as shown in the left panel of Fig. 2, for $\gamma = 0.51$, P is centered around negative values of the magnetization m_Z. With increasing J, the distribution P shifts towards more negative values. Therefore, as soon as γ is different from $\frac{1}{2}$, the effects of the bath induce a finite magnetization along the z axis. QMC results for $\gamma \neq \frac{1}{2}$ can be better understood through the VMF approach, exposed below, in terms of a dissipation-induced magnetic field along the z axis. On the other hand, interactions between spins and classical baths preserve Z_2 symmetry, therefore, as shown in the right panel of Fig. 2, the function P bears some resemblance with the distribution function shown in the right panel of Fig. 1 at $\gamma = \frac{1}{2}$. We stress the prominent link between Z_2 symmetry and magnetic properties in the case of quantum/classical baths with varying γ.

The values of the bath parameter γ smaller than $\frac{1}{2}$ favor positive values of the magnetization along the z axis. In fact, configurations with opposite values of m_z are obtained for values of γ symmetric around $\frac{1}{2}$. For example, at $\gamma = 0.49$ and fixed α, the distribution function P can be obtained from that shown in the left panel of Fig. 2, making only the transformation $m_Z \to -m_Z$. In order to interpret in a more effective way the numerically exact QMC results, in the following we will present a zero-temperature VMF approach within the framework of the spin polaron [13].

VMF: Spin polaron framework. The trial wave function is $|\psi\rangle = \prod_{i=1}^{L} |\psi_i\rangle$, where $|\psi_i\rangle$ represents the wave function of a single spin interacting with its local bath. The single-spin polaron will be variationally addressed for both classical and quantum baths. We simplify the notation for $L = 1$ in Eq. (1): $\sigma_i^x = \sigma_x$, $\sigma_i^z = \sigma_z$, $\sigma_i^+ = \sigma_+$, $\sigma_i^- = \sigma_-$, and, consequently, $a_{i,k}^+ = a_k^+$, $a_{i,k} = a_k$.

First, we use the adiabatic approximation, rigorously valid in the classical limit. Indeed, the wave function of the system can be factorized into a product of normalized variational

functions $|\varphi\rangle$ and $|g\rangle$, depending on the spin and bosonic coordinates, respectively: $|\psi\rangle = |\varphi\rangle|g\rangle$. The expectation value of the Hamiltonian (1) on the state $|\varphi\rangle$ provides an effective Hamiltonian for the bath whose ground wave function is a coherent state:

$$|g\rangle = e^{\sum_k \left(\frac{f\lambda_k}{\omega_q} a_k - \text{H.c.}\right)}|0\rangle. \tag{7}$$

Here, $|0\rangle$ is the bosonic vacuum state and $f = \langle\varphi|[(1-\gamma)\sigma_+ + \gamma\sigma_-]|\varphi\rangle$. At this stage, the bosonic state $|g\rangle$ can be used to obtain an effective Hamiltonian H_{eff} for the spin. It is straightforward to show that $H_{\text{eff}} = -\frac{\tilde{\Delta}}{2}\sigma_x + C$, where $\tilde{\Delta} = 1 + \sum_k \frac{2f\lambda_k^2}{\omega_k}$ and $C = \sum_k \frac{f^2\lambda_k^2}{\omega_k}$, i.e., the adiabatic approximation leads only to an enhancement of the transverse magnetic field along the x axis, which is, however, enough to interpret the QMC results at $\gamma = \frac{1}{2}$, shown in Fig. 1.

In order to get a proper inclusion of the quantum nonadiabatic contributions, relevant for $\gamma \neq \frac{1}{2}$, we first apply a unitary transformation $H_1 = e^{S_1} H e^{-S_1}$, with $S_1 = -\sum_k (\frac{f\lambda_k}{\omega_k} a_k - \text{H.c.})$, as suggested by Eq. (7). The transformed Hamiltonian assumes the form

$$H_1 = H_{\text{eff}} + \sum_q \omega_k a_k^\dagger a_k + \tilde{H}_I, \tag{8}$$

where $\tilde{H}_I = \sum_k \lambda_k A a_k + \text{H.c.}$, A being an operator acting only on the spin subsystem: $A = [(1-\gamma)\sigma_+ + \gamma\sigma_-] - f$. By treating $\tilde{H}_I$ as perturbation, one includes the nonadiabatic contributions. The first order of the perturbation theory, followed by the assumption of no correlation between the emission of different bosons, suggests the following trial state for the bath: $e^{-S_2}|0\rangle$, where $S_2 = -\sum_k \sigma_z(\frac{f_1\lambda_k}{\omega_k+\tilde{\Delta}} a_k - \text{H.c.})$ and $f_1 = \gamma - 1/2$. In other words, S_2 takes into account the possibility that the bath can follow instantaneously the spin oscillations. The effective Hamiltonian for the spin turns out to be

$$H_{\text{eff}} = -\frac{\Delta_{\text{eff}}}{2}\sigma_x + C_{\text{eff}} + h_{\text{eff}}\sigma_z, \tag{9}$$

where $\Delta_{\text{eff}} = (\tilde{\Delta} + \sum_k \frac{4f_1^2\lambda_k^2}{\omega_k+\tilde{\Delta}})e^{-\sum_k \frac{2f_1^2\lambda_k^2}{(\omega_k+\tilde{\Delta})^2}}$ is the effective transverse magnetic field, $C_{\text{eff}} = C + \sum_k \frac{\omega_k f_1^2\lambda_k^2}{(\omega_k+\tilde{\Delta})^2}$ is a constant, and $h_{\text{eff}} = 2f\sum_k \frac{f_1\lambda_k^2}{\omega_k+\tilde{\Delta}}$ is the effective longitudinal magnetic field. It is evident that the quantum fluctuations of the bath induce a field h_{eff} along the z axis that breaks the Z_2 symmetry. Moreover, the field h_{eff} changes sign with crossing $\gamma = \frac{1}{2}$. We note that the parameter f_1 is relevant for γ different from $1/2$. Indeed, h_{eff} is proportional to the product of the parameters f and f_1.

The VMF approach can be further improved by diagonalizing the original Hamiltonian in the subspace spanned by the following $2M$ wave functions, $\psi_i = e^{\sum_k (l_{k,i}a_k - \text{H.c.})}|0\rangle|\uparrow\rangle$ and $\phi_i = e^{\sum_k (h_{k,i}a_k - \text{H.c.})}|0\rangle|\downarrow\rangle$, with $i = 1, \ldots, M$, in analogy with approaches for polaronic models [26–30]. Here, as suggested by the above described approach, we assume $l_{k,i} = \frac{f\lambda_k}{\omega_k} + \frac{\lambda_k f_i}{\omega_k+\Delta_i}$, $h_{k,i} = \frac{f\lambda_k}{\omega_k} - \frac{\lambda_k f_i}{\omega_q+\Delta_i}$, with f, f_i, and Δ_i $2M+1$ variational parameters. In Figs. 3(a) and 3(b), where we successfully compare the calculated magnetization m_Z with QMC results for the single spin, we prove that $M = 2$ is enough to get a very accurate description of the spin polaron in any regime. Moreover, in the case of a single spin, as expected, the magnetization vanishes at $\gamma = \frac{1}{2}$, and, as a function of γ, shows a crossover behavior, weakly dependent on α, from positive to negative values.

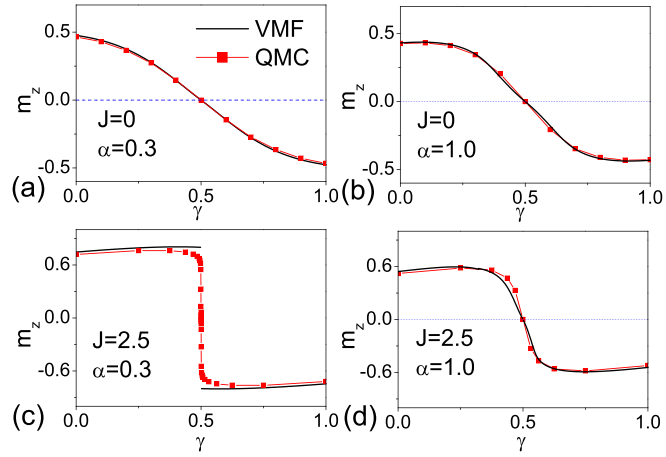

FIG. 3. Magnetization m_Z as a function of γ for different values of J and α by using both QMC and VMF methods. Simulation parameters: $\beta = 100$ for QMC, $T = 0$ for VMF; $L = 1$ (single spin) in (a) and (b) for QMC and VMF, $L = 40$ in (c), and $L = 10$ in (d) for QMC, L very large for VMF in (c) and (d).

In the case of a spin chain, as shown in Figs. 3(c) and 3(d), the calculated magnetization m_Z perfectly matches QMC results for J larger than J_C [Fig. 3(c), $\alpha = 0.3$, $J_C = 2.47$ at $\gamma = \frac{1}{2}$] and smaller than J_C [Fig. 3(d), $\alpha = 1$, $J_C = 3.63$ at $\gamma = \frac{1}{2}$]. In the first case, there is an actual first-order transition induced by γ between states with opposite magnetization, while in the second case, only a crossover takes place at $\gamma = \frac{1}{2}$. We stress that the first-order transition does take place only for values of J larger than the critical J_c obtained at $\gamma = 1/2$. Moreover, we remark that the first-order transition occurs also for lower values of α, therefore the spin system shows a large sensitivity to external perturbations even at minimal coupling [21].

Finally, we complement the phase diagram of Fig. 1, showing in Fig. 4 the diagram with γ vs α at fixed J (left panel), and

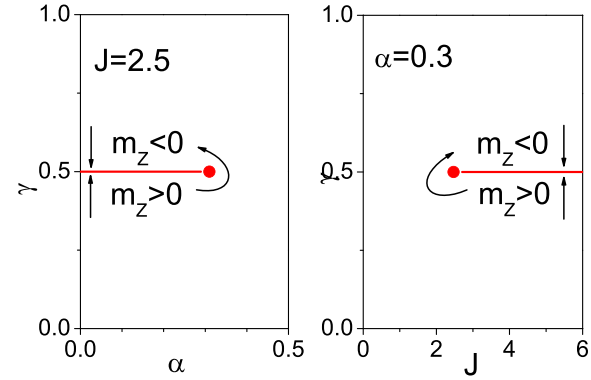

FIG. 4. Phase diagram with γ vs α at $J = 2.5$ (left panel), with γ vs J at $\alpha = 0.3$ (right panel). Vertical arrows indicate first-order transitions, and circles denote second-order critical points which can be encircled (curved arrows). QMC simulation parameters: $\beta = 100$, $L = 40$.

the diagram with γ vs J at fixed α (right panel). It is apparent that one gets a horizontal line at $\gamma = \frac{1}{2}$ of first-order transitions terminating with a second-order critical point (denoted with a circle in the panels of Fig. 4). From the comparison with the phase diagram in Fig. 1, the critical point at $\alpha = 0.3$ in the right panel corresponds to $J_c = 2.47$. As expected in this kind of transition [1], one can go continuously from a magnetization state to its opposite encircling the second-order critical point (curved arrows).

Conclusions. In this Letter, through a numerically exact QMC method and VMF approach, we have shown that a combination of Jaynes-Cummings and anti-Jaynes-Cummings spin-bath local couplings drives the transition in a transverse field Ising chain from the second to the first order even for a low dissipation strength α. Actually, first-order transitions are obtained by varying the additional parameter γ, which modulates the relative coupling between Jaynes-Cummings and anti-Jaynes-Cummings terms. We stress that, in the absence of the parameter γ, as reported for example in a previous study [14], a global boson bath promotes quantum phase transitions which are continuous and start from a critical value of α.

In addition to spin-spin interactions [9,10], Jaynes-Cummings couplings can be implemented in quantum simulators [31,32], which, therefore, can potentially test the results exposed in this Letter. Moreover, one can exploit the high sensitivity of the systems near the transition point of first-order quantum transitions [2], which are found to be robust against dissipation [33]. Indeed, for values of γ close to 0.5, the magnetization is sensitive to the variation of J (hence of the magnetic field Δ). Therefore, the quantum bath engineering gives rise to a setup which can be relevant for the realization of small-scale quantum sensors. Finally, the approaches used in this Letter can be easily generalized to more complex spin systems [34,35] and spin-bath couplings [36], and in principle allow us also to include the effects of coherent sinusoidal drives [37].

Acknowledgments. V.C. and G.D.F. acknowledge a critical reading of the manuscript by N. Nagaosa. This work was supported by PNRR MUR Project No. PE0000023-NQSTI.

[1] S. Sachdev, *Quantum Phase Transitions*, 2nd ed. (Cambridge University Press, Cambridge, UK, 2011).
[2] D. Rossini and E. Vicari, Phys. Rep. **936**, 1 (2021).
[3] S. Suzuki, J. Inoue, and B. K. Chakrabarti, *Quantum Ising Phases and Transitions in Transverse Ising Models*, 2nd ed. (Springer, Berlin, 2012).
[4] L. M. Sieberer, M. Buchhold, and S. Diehl, Rep. Prog. Phys. **79**, 096001 (2016).
[5] H.-P. Breuer and F. Petruccione, *The Theory of Open Quantum Systems* (Oxford University Press, New York, 2007).
[6] A. O. Caldeira and A. J. Leggett, Ann. Phys. **149**, 374 (1983).
[7] A. J. Leggett, S. Chakravarty, A. T. Dorsey, M. P. A. Fisher, A. Garg, and W. Zwerger, Rev. Mod. Phys. **59**, 1 (1987).
[8] H.-P. Breuer, E.-M. Laine, J. Piilo, and B. Vacchini, Rev. Mod. Phys. **88**, 021002 (2016).
[9] H. Bernien, S. Schwartz, A. Keesling, H. Levine, A. Omran, H. Pichler, S. Choi, A. S. Zibrov, M. Endres, M. Greiner, V. Vuletic, and M. D. Lukin, Nature (London) **551**, 579 (2017).
[10] A. Keesling, A. Omran, H. Levine, H. Bernien, H. Pichler, S. Choi, R. Samajdar, S. Schwartz, P. Silvi, S. Sachdev, P. Zoller, M. Endres, M. Greiner, V. Vuletic, and M. D. Lukin, Nature (London) **568**, 207 (2019).
[11] S. Ebadi1, T. T. Wang, H. Levine, A. Keesling, G. Semeghini, A. Omran, D. Bluvstein, R. Samajdar, H. Pichler, W. W. Ho, S. Choi, S. Sachdev, M. Greiner, V. Vuletic, and M. D. Lukin, Nature (London) **595**, 227 (2021).
[12] C. Noh and D. G. Angelakis, Rep. Prog. Phys. **80**, 016401 (2017).
[13] K. Le Hur, in *Understanding Quantum Phase Transitions*, edited by L. D. Carr (CRC Press, Boca Raton, FL, 2010).
[14] G. De Filippis, A. de Candia, A. S. Mishchenko, L. M. Cangemi, A. Nocera, P. A. Mishchenko, M. Sassetti, R. Fazio, N. Nagaosa, and V. Cataudella, Phys. Rev. B **104**, L060410 (2021).
[15] G. De Filippis, A. de Candia, G. Di Bello, C. A. Perroni, L. M. Cangemi, A. Nocera, M. Sassetti, R. Fazio, and V. Cataudella, arXiv:2205.11555.
[16] P. Werner, M. Troyer, and S. Sachdev, J. Phys. Soc. Jpn. **74**, 67 (2005).
[17] P. Werner, K. Volker, M. Troyer, and S. Chakravarty, Phys. Rev. Lett. **94**, 047201 (2005).
[18] P. Werner and M. Troyer, Prog. Theor. Phys. Suppl. **160**, 395 (2005).
[19] G. M. Uhdre, D. Cius, and F. M. Andrade, Phys. Rev. A **105**, 013703 (2022).
[20] J. A. Omolo, arXiv:2103.09546.
[21] See Supplemental Material at http://link.aps.org/supplemental/10.1103/PhysRevB.107.L100302, for additional details about the QMC method, expanding not only the limit of classical bath oscillators, but introducing also Binder cumulants, which are used to evaluate the phase diagram shown in Fig. 1, and for a discussion on the finite-size scaling of the magnetization m_Z in the parameter regime of Fig. 3(c) and the interesting behavior of the magnetization m_X for the same parameters as in Fig. 3, which includes Refs. [3,17,38,39].
[22] U. Weiss, *Dissipative Quantum Systems*, 4th ed. (World Scientific, Singapore, 2012).
[23] I. B. Sperstad, E. B. Stiansen, and A. Sudbo, Phys. Rev. B **81**, 104302 (2010).
[24] We have checked that our method perfectly reproduces the QMC results reported in Ref. [17].
[25] In the case of single-spin and Ohmic baths, a mapping to the Kondo problem can be typically done [22]. Magnetic transitions in the Kondo model can be used to accurately predict the localized-delocalized phase transition of the Kosterlitz-Thouless type in the original spin-boson model. In our model, for the case of a single spin, there is not a Kosterlitz-Thouless-type transition, making the mapping to the Kondo model useless.

[26] C. A. Perroni, A. Nocera, V. M. Ramaglia, and V. Cataudella, Phys. Rev. B **83**, 245107 (2011).
[27] F. Gargiulo, C. A. Perroni, V. M. Ramaglia, and V. Cataudella, Phys. Rev. B **84**, 245204 (2011).
[28] C. A. Perroni, F. Romeo, A. Nocera, R. Citro, and V. Cataudella, J. Phys.: Condens. Matter **26**, 365301 (2014).
[29] C. A. Perroni, A. Nocera, and V. Cataudella, Europhys. Lett. **103**, 58001 (2013).
[30] C. A. Perroni, D. Ninno, and V. Cataudella, New J. Phys. **17**, 083050 (2015).
[31] J. S. Pedernales, I. Lizuain, S. Felicetti, G. Romero, L. Lamata, and E. Solano, Sci. Rep. **5**, 15472 (2015).
[32] J. Braumüller, M. Marthaler, A. Schneider, A. Stehli, H. Rotzinger, M. Weides, and A. V. Ustinov, Nat. Commun. **8**, 779 (2017).
[33] M. Raghunandan, J. Wrachtrup, and H. Weimer, Phys. Rev. Lett. **120**, 150501 (2018).
[34] J. Jin, W.-B. He, F. Iemini, D. Ferreira, Y.-D. Wang, S. Chesi, and R. Fazio, Phys. Rev. B **104**, 214301 (2021).
[35] M. Weber, D. J. Luitz, and F. F. Assaad, Phys. Rev. Lett. **129**, 056402 (2022).
[36] Y. Zheng and S. Yang, Phys. Rev. A **104**, 023304 (2021).
[37] H. Landa, M. Schiró, and G. Misguich, Phys. Rev. Lett. **124**, 043601 (2020).
[38] M. Guo, R. N. Bhatt, and D. A. Huse, Phys. Rev. Lett. **72**, 4137 (1994); H. Rieger and A. P. Young, *ibid.* **72**, 4141 (1994).
[39] V. Cataudella, G. De Filippis, F. Martone, and C. A. Perroni, Phys. Rev. B **70**, 193105 (2004).